Available online at www.sciencedirect.com

ScienceDirect

Energy Procedia 4 (2011) 2340–2347

Energy Procedia

www.elsevier.com/locate/procedia

GHGT-10

Effect of contaminants on the thermodynamic properties of CO_2-rich fluids and ramifications in the design of surface and injection facilities for geologic CO_2 sequestration

S. Verma, C. S. Oakes, N. Chugunov, and T. S. Ramakrishnan

Schlumberger–Doll Research Laboratory, Cambridge, MA 02139, USA

Abstract

Geologic storage may involve injection of impure carbon dioxide (CO_2) streams in order to lower capture costs. The contaminants in the purified CO_2 stream depend on the type of power plant and the capture scheme. For on oxy-fuel based combustion cycle, we have previously evaluated the effect of presence of oxygen, nitrogen and argon on the CO_2 phase diagram and the critical properties of mixtures in these systems [1].

For a 320 km pipeline, we established a base case for pure CO_2, and evaluated the difference in compressor power requirements as each contaminant was added in fixed proportions [1]. The key finding was that if the mixture encountered a two-phase region along the pipeline, the pressure drop becomes punitive. We proposed a minimal adjustment of operating conditions (or the temperature and pressure profile along the pipeline) to avoid the two-phase region and concomitant prohibitive pressure losses. In this paper, we consider the influence of hydrogen sulfide and water on the phase behavior of the CO_2-rich captured stream. Specifically, we examine the phase equilibria and the PVT properties, and compare the GERG–2008 equation of state (EoS) computations with experimental data.

In general, CO_2-rich effluent mixtures from oxy-fuel plants may undergo phase separation at higher pressures than that for pure CO_2 for the temperature range likely to be encountered in surface and injection facilities designed for CO_2 sequestration. In addition, density, compressibility, and reactive properties of these mixtures may be significantly different from pure CO_2. Consequently, operation of large geologic CO_2 storage sites must anticipate how these differences in the thermodynamic properties of the injected fluids may affect compressor power requirements, pipeline transport, well design, and wellbore and reservoir integrity.

Keywords: Carbon dioxide (CO_2), Hydrogen sulfide (H_2S), water (H_2O), pressure drop, pipeline.

1. Introduction

For economic reasons, geologic storage may involve injection of impure CO_2-streams. The contaminants in the purified CO_2 stream depend on the type of power plant and capture scheme. For example, flue gases from an oxy-combustion power plant are likely to contain contaminants such as argon, nitrogen and oxygen. If the power plant is

doi:10.1016/j.egypro.2011.02.125

based on integrated gasification combined cycle (IGCC) technology, then the captured stream is likely to contain elevated levels of H_2S and carbon monoxide. Conversely, an effluent gas stream from a post-combustion capture unit contains small amounts of SO_x, NO_x, oxygen and nitrogen. H_2O is present as a contaminant in flue gases from all sources, regardless of the source-type, and is removed to acceptable levels in order to prevent corrosion and adverse levels of CO_2 reactivity.

With emphasis on an oxy-fuel system, we previously evaluated the effect of oxygen, nitrogen and argon on the CO_2 phase diagram [1]. Each of the three contaminants exhibit a Type I critical curve behavior in binary mixtures with CO_2. The critical pressure increases relative to pure carbon dioxide while the critical temperature of each mixture is lower than the critical temperature of pure carbon dioxide. In the present paper, we consider H_2S and H_2O as impurities in the captured stream and evaluate the effect of these contaminants on the phase behavior.

Specifically, we examine the effect of the two contaminants on phase equilibria and PVT properties of a CO_2-rich fluid and compare the predictions of GERG–2008 equation of state (EoS) to published experimental data. The GERG–2008 EoS for mixtures has been fit by its developers to a variety of systems relevant to CO_2 capture and storage including mixtures containing N_2, O_2, Ar, H_2S, CH_4, and H_2O. The model has the capability to accurately reproduce the thermodynamic properties of compositionally complex fluids, including dense liquids, through parameter sets obtained only from unary and binary component systems. However, for some systems, there are data at different pressures, temperatures, compositions and for different thermodynamic property types than were used to parameterize the model. Thus, the model can be tested against data not used for parameterization. We demonstrate compositional and property ranges where the model is accurate, and where agreement with experiment deteriorates.

In our previous paper [1] we also examined the effect of contaminant addition to pipeline design and operation. For a 320 km long pipeline, we established a base case for pure CO_2, and evaluated the difference in compressor power requirements as each contaminant was progressively added in fixed proportions. The key finding was that if the mixture entered the two-phase envelope along the pipeline, then the pressure drop was punitive. We proposed a minimal adjustment of operating conditions (or the temperature and pressure profile along the pipeline) to avoid the two-phase region and concomitant prohibitive pressure losses. Using the mixture phase diagrams, optimal pressure profiles along the pipeline were generated for all binary mixtures with CO_2 as the major component. This has now been extended for the presence of H_2S and water vapor in the captured CO_2-rich streams.

In general, mixtures may undergo phase separation at higher pressures than the critical pressure of pure CO_2 and at temperatures likely to be encountered in surface and injection facilities. In addition, density, compressibility, and reactive properties of these mixtures may be significantly different from pure CO_2. Hence, operation of geologic CO_2 storage sites must anticipate how these differences in the thermodynamic properties of the injected fluids may affect compressor power requirements, pipeline transport, well design, and wellbore and reservoir integrity.

2. Review of available carbon dioxide pipeline specifications for hydrogen sulfide and water

There are many proposed specifications available for pipeline quality carbon dioxide, a compilation of which is presented in Table 1 [2–13]. Since a pipeline network shared between various sources and sinks has not yet evolved, regulations for pipeline quality carbon dioxide do not exist. The specifications summarized in Table 1 are mostly for operators with dedicated pipelines based on their experience, available thermodynamic data and regulations outside of CO_2 storage, e.g. concern for atmospheric leaks, corrosion etc. In some cases, the specifications are based on natural sources of carbon dioxide and its composition. Most of the existing pipelines for carbon dioxide are used enhanced oil recovery (EOR). Therefore, there is little distinction between the composition of the natural supply, pipeline specification, and the operational oilfield injection composition. For storage application, in the absence of regulations, the composition is dictated by the power generation process, the capture method, and the operational efficiency penalty. For example, if the CO_2 source is an IGCC plant followed by a conventional amine scrubbing system, the CO_2 specification will provide reasonable limits on hydrogen, carbon monoxide and hydrogen sulfide as these are likely to be the main contaminants. Conversely, effluent specifications for an oxy-fuel power plant are likely to allow elevated levels of argon, oxygen, and perhaps nitrogen.

Most pipeline specifications specify a minimum CO_2 purity of 95% although there are two that relax this to 90%. Some specifications require almost pure (or greater than 98%) CO_2. Almost all of the specifications that require a high CO_2 purity are for naturally produced CO_2. C2 and higher hydrocarbons are limited to approximately 2–2.3% in the specifications that provide a guideline. There is significantly more variation in the CO limits; specifications

range from 0.1% to 4% with Alstom providing the highest limit. Total hydrocarbons, a separate listing, are limited to 5% in some of the specifications. Hydrogen limits vary from 0.1% to 4%. Methane concentrations are almost similar to total hydrocarbons and are limited to 5% by volume suggesting that the primary hydrocarbon constituent considered is methane. Only two of the tabulated specifications provide a limit for NO_x, with an upper limit of 1500 ppm. The limits on SO_x, range from 2 ppm to 1500 ppm. NO_x and SO_x emissions from power plants are strictly regulated, and most operating power plants have treatment facilities to limit their concentrations in the effluent stream. The mandated limits are likely to be the same for transport to a storage site.

Oxygen limit is specified ranging from 10 ppm to 4% by volume. The flue gas from a power plant operating in an oxidizing environment, where combustion commonly takes place in excess oxygen or air, is likely to contain oxygen in the 1–2% range. The other key constituent likely in these effluent streams is nitrogen; the limits specified vary from 0.03% to 4% by volume. Argon is limited to 4% by volume in the few instances where it is listed.

Safety reasons dictate low H_2S concentration in CO_2 rich streams for pipeline transport. Most specifications provide limits for hydrogen sulfide and these vary greatly from 70 ppm to 1.5% by volume. The TLV/TWA (threshold limit value for the time weighted average in an eight hour day and 40 hour week) is as low as 10 ppm although at 5 ppm exposure induced effects are noticeable [31]. H_2S is likely to exist in effluent streams from IGCC plants or where carbon based fuels are transformed to low energy products in a reducing environment and in natural sources of CO_2.

Most specifications also provide limits for water concentration and these limits range from 2–641 ppm. All sources of purified carbon dioxide are likely to contain water. Post compression, water levels are reduced to saturated conditions which are a function of temperature and pressure. For example, if a CO_2 stream is compressed from ambient pressure to 200 bar, and subsequently cooled to 35 °C for injection, the mole fraction of water in this stream is 0.0015 (or 1502 ppm or 71.36 lbs/MMSCF). This water content may then be reduced to acceptable levels by use of a suitable dehydration technique prior to transportation in a pipeline.

3. Unary CO_2 system

A phase diagram for pure carbon dioxide is shown in Figure 1 [14]. The CO_2 vapor–liquid equilibrium curve extends from the triple point at 216 59 K and 0.518 MPa to the critical point at 304.13 K and 7.377 MPa. Span and Wagner [14] reviewed the plethora of data for the unary system and constructed a high accuracy (reference) equation of state valid from 217 K to 1100 K and 800 MPa.

A few sources of thermodynamic data have been published subsequent to the Span-Wagner EoS [15–17].

4. CO_2–H_2S mixtures

The most recent PVT and phase equilibrium data for this system that we are aware of are in Stouffer et al. [18] and Zhang et al. [19]. Earlier data sources are referenced in these papers.

With the exception of the density data of Stouffer et al. [18] and Bailey et al. [20] and the enthalpy data of Barry et al. [21] there are no data outside of the *P–T* region bounded by the unary system vapor–liquid equilibrium (VLE) curves and the binary system critical curve. We are not aware of any thermodynamic data for this system above ≈20 MPa and for densities greater than those corresponding to the highest density isochore measured by Bailey et al. [20] (Figure 3). Consequently, calculations of thermodynamic properties of homogenous, high-density CO_2+H_2S mixtures above 20 MPa may not be accurate. The *P–T* region lacking data encompasses conditions likely to exist in some CO_2 sequestration reservoirs.

Figure 4 shows a few bubble-point and dew-point curves calculated using Refprop 8.1b and the GERG–2008 model corresponding to X_{H2S} compositions which may be produced by an IGCC plant. This is a simple Type 1 system with a continuous critical curve between the critical end-points of the unary systems. While not explicitly shown here, for $X_{CO2} > 0.9$, co-existing liquid and vapor phases have nearly identical compositions.

5. CO_2–H_2O phase diagram

The CO_2+H_2O system has a large *P–T–X* region of fluid immiscibility and solid–fluid equilibria under conditions relevant to CO_2 sequestration. The phase equilibrium topology and sources of PVTX data have been reviewed and

presented in numerous publications [22–28]. Recent measurements of thermodynamic properties for this system include those of Novitskiy et al. [29] and Siqueira-Campos et al. [30].

While the GERG–2008 EoS includes model parameters for the CO_2+H_2O system, it should be noted that only two data sources were used to establish those parameters and those sources contain only density data. Consequently, the GERG–2008 EoS does not accurately reproduce fluid phase equilibria for this system at the low end of the claimed range of validity (c.f. Figure 5, 348 K). However, it is a remarkable attribute of the model that the calculated form of the phase envelope is correct even though phase equilibria was not used to parameterize the model.

If water concentrations exiting the compressor are allowed to exceed $X_{CO2} \approx 0.001$, then CO_2-hydrate may form in some parts of the surface infrastructure [24, 27]. Hydrate may accumulate and upon melting raise the local water concentration to the point where liquid water pools or accumulates in crevices thereby posing a corrosion hazard.

6. Pipeline Model

Figure 2 shows a simplified schematic for carbon dioxide sequestration. A purified stream of carbon dioxide is compressed and then cooled in an after-cooler (or a heat exchanger that may be air or water cooled). This stream with pressure P_i, temperature T_i and mole fraction X_i forms the inlet stream to the pipeline. The pipeline considered in our analysis is 320 km long. The considered pipeline configuration is 16 km buried in the ground followed by 16 km of pipeline elevated above the ground. The remainder of the pipeline, or 288 km is buried in the ground. The ambient temperature is 15.6 °C (60 ºF). The CO_2 flow rate is set at one million (short) tons per year. The default pipeline diameter is 12”(≈30cm). Purified CO_2 stream is introduced into the pipeline at 37.7 °C. Frictional pressure drop in the pipeline is calculated using the Beggs and Brill and, in some instances, the OLGA S correlations. To complete the presented schematic, outlet conditions from the pipeline are pressure P_o, temperature T_o and mole fractions X_o. This outlet stream is injected downhole for sequestration.

Figure 6 shows the vapor fraction, temperature, and pressure for the CO_2 stream along the pipeline. Our simulator treats the supercritical state as a vapor fraction of unity; therefore the changeover in vapor fraction from one to zero signals the supercritical to liquid transition. In principle, the profile for this transition should be sharp, since there is no latent heat associated with this change. The Beggs and Brill correlation captures this accurately. The temperature of the carbon dioxide stream gradually cools to the ambient temperature as it moves along the pipeline. At an ambient temperature of 15.6 ºC, the pressure of this stream drops about 4.1% for the 18” (≈45 cm) pipeline and 25% for the 12” pipeline from an inlet pressure of 8.27 MPa. For each pipe diameter, this is close to the minimum pressure drop, given that there is no phase transition. When the ambient temperature is changed to 23.9 °C (75 °F) for the 12” pipeline, the fluid goes from supercritical to liquid along the pipeline as in the previous two instances. However, at about the 200 km mark, vapor formation is initiated and the vapour fraction subsequently exceeds 40% at the pipeline outlet. The outlet temperature drops to about 10 °C and the pressure drop along the pipeline is 42.5% of the inlet pressure. This effect is explained in more detail below.

The effect of adding 4% (mol) H_2S to the carbon dioxide is considered in Figure 7. The inlet pressure to the pipeline is set at 8.27 MPa (1200 psia) as for the pure carbon dioxide stream. The vapor fraction behavior is similar to that for pure CO_2 in that the mixture goes from the supercritical region to the liquid region along the pipeline. The temperature and pressure profiles along the pipeline are also similar to those for pure carbon dioxide. The outlet pressure is about 6.3 MPa, just slightly lower than for pure CO_2 and the outlet temperature is 15.5 °C. This result is not unexpected because the mixture viscosity and density for the CO_2–H_2S mixture containing 4% (mol) H_2S is very close to those of pure CO_2.

Figure 7 also shows the results of introducing the 4% (mol) H_2S gas mixture to the pipeline at a pressure of 7.58 MPa (1100 psia). The vapor fraction of this gas mixture, as for previous simulations, is initially in the supercritical region and then approaches the vapor–liquid curve. As the pressure drops along the pipeline, the mixture tends to promote vapor formation. Concurrently, due to heat transfer to the ambient, the reduction in temperature favors liquid formation. These competing effects initially lead to liquid formation, but at pipeline lengths greater than 200 km, vapor formation is increased. This has a direct effect on the pressure and temperature profiles along the pipeline. The enthalpy change associated with vapor formation (or the latent heat of vaporization) leads to a temperature reduction, while the two phase flow (liquid–vapor flow as opposed to supercritical–liquid

flow) leads to additional frictional loss. The latter has a positive feedback, leading to progressively larger vapor fraction.

The pressure–temperature profile along the pipeline for CO_2–H_2S mixture is shown on the CO_2–H_2S phase diagram (in the *P–T* plane as shown in Figure 8). The total H_2S content in the vapour and liquid phases is constant at 4% (mol). The profile for an inlet pressure of 1200 psia, as discussed previously starts in the supercritical region and gradually moves into the liquid region. For an inlet pressure of 1100 psia, the mixture also starts off in the supercritical region, passes close to the critical point and then follows the vapor–liquid line until the outlet of the pipeline. Conceivably, if the pipeline had been longer, the mixture may have transitioned completely into the vapor region.

The effect of water addition to CO_2 was also simulated. However, since the water content of the CO_2 stream is limited to 0.0032 mole%, there was no observable impact of water vapor on the temperature or pressure profile along the pipeline.

7. Results and conclusions

A review of available pipeline specifications for limits on contaminants in carbon dioxide transported in pipeline shows considerable variation. The variation arises largely as a result of source diversity. The compositional variation, especially under near critical conditions has a strong influence on the pressure drop. Therefore pipeline models must take into account composition of the feed-stream and the corresponding equation of state for operational design.

The unary carbon dioxide thermodynamic properties are accurately described by the GERG–2008 EoS. The GERG–2008 model also accurately reproduces VLE for the binary mixture of CO_2 and H_2S; however, data for this system at pressures above 20 MPa are sparse, and the GERG–2008 EoS may not accurately reproduce PVT properties of single-phase high-density mixtures. GERG–2008 does not currently reproduce low temperature fluid equilibria below 373 K accurately; however, sufficient data exist so that re-parameterization of the model may resolve this problem.

In the supercritical region or the liquid state, the pressure drop in the pipeline is relatively low. If the carbon dioxide stream touches the vapor–liquid phase boundary or crosses over to the vapor region, the frictional pressure drop become prohibitive. For a given wellhead pressure, a higher pressure drop translates to a higher outlet pressure from the compressor and therefore, a higher power consumption by the compressor. It is therefore desirable to design and operate a pipeline such that the carbon dioxide stays as a liquid or a supercritical fluid throughout the length of the pipeline.

Unlike N_2, Ar, and O_2, addition of small quantities of H_2S to CO_2 do not significantly enlarge the P–T region of fluid immiscibility (Figure 9). Consequently, H_2S is of lesser concern with regard to phase equilibrium effects on compression requirements.

References

1. Verma S., Oakes C., Ramakrishnan T. S., Harichandran A., Peters D. (2009) Effect of contaminants on thermodynamic properties of carbon dioxide and ramifications in the design of surface facilities for geologic sequestration. DOE NETL 8th Annual Conference on Carbon Capture & Sequestration, May 4th – 7th, 2009, Pittsburgh, PA.
2. Air Products. White, V. (2008) CO_2 Quality for Storage: Technical Barriers. http://www.co2captureandstorage.info/docs/oxyfuel/3rd%20Mtg/04-02%20V.%20White%20(Air%20Products).pdf
3. Alstom. Wolf, M., G. Kaefer (2007) CO_2 purity required for carbon capture & storage. EU ZEP meeting. Dec. 6th, 2007.
4. APGTF – Advanced Power Generation Technology Forum. (2002) Carbon dioxide capture and storage. pg 48. http://www.dti.gov.uk/files/file21933.pdf
5. CoalFleet (2008). CoalFleet User Design Basis Specification for Coal Based Integrated Gasification Combined Cycle (IGCC) Power Plants. EPRI. Version 8. 1014215 Technical Update. July 22, 2008. Pg 10–24 to 10–55.
6. Dakota Gasification Company http://www.dakotagas.com/Miscellaneous/pdf/Safety_ByproductInfo/SpecSheets/co2spec.pdf

7. Dynamis. E. de Visser (2007) Dynamis – Ecofys Netherlands. The 4th Trondheim Conference on CO2 Capture, Transport and Storage. October 16 – 17, 2007, Trondheim Norway. http://www.energy.sintef.no/arr/CO2_2007/index.asp
8. Elsam A/S; Kinder Morgan CO2 Company L.P.; New Energy, Statoil (2003). http://www.co2.no/download.asp?DAFID=17&DAAID=6
9. GE GR – Munich. Finkenrath, Matthias (GE, Research)
10. IEA GHG Weyburn – CO_2 monitoring and storage project. Petroleum Technology Research Center. http://www.ieagreen.org.uk/glossies/weyburn.pdf
11. IPCC Special Report (2005) Carbon dioxide capture and storage. Intergovernmental Panel of Climate Change. http://www.ipcc.ch/publications_and_data/publications_and_data_reports.htm
12. Kinder Morgan. (2006) CAPP investment symposium. http://capp.ca/raw.asp?x=1&dt=PDF&dn=104965
13. Oosterkamp A., Ramsen J., Seevam P., Race J. and Downie M. (2007) Pipeline transport of CO_2 with impurities – a state of the art review. Polytec. http://www.energy.sintef.no/arr/CO2_2007/index.asp
14. Span R. and Wagner, W. (1996) A New Equation of State for Carbon Dioxide Covering the Fluid Region from the Triple-Point Temperature to 1100 K at Pressures up to 800 MPa. *J. Phys. Chem. Ref. Data* **25**, 1509–1596.
15. Estrada-Alexanders A.F. and Trusler J.P.M. (1998) Speed of sound in carbon dioxide at temperatures between (220 and 450) K and pressures up to 14 MPa. *J. Chem. Thermo*. **30**, 1589–1601.
16. Gil L., Otín S.F., Embid J.M., Gallardo M. A., Blanco S., Artal M. and Velasco I. (2008) Experimental setup to measure critical properties of pure and binary mixtures and their densities at different pressures and temperatures Determination of the precision and uncertainty in the results. *J. Supercrit. Fluids* **44**, 123–138.
17. Mantilla I. D., Cristancho D. E., Ejaz S., Hall K. R., Atilhan M. and Iglesias-Silva G. A. (2010) P–ρ–T Data for Carbon Dioxide from (310 to 450) K up to 160 MPa. *J. Chem. Eng. Data* in press.
18. Stouffer C. E., Kellerman S. J., Hall K. R., Holste J. C., Gammon B. E. and Marsh K. N. (2001) Densities of carbon dioxide + hydrogen sulfide mixtures from 220 K to 450 K at pressures up to 25 MPa. *J. Chem. Eng. Data* **46**, 1309–1318.
19. Zhang J., Zhang X., Han B., He J., Liu Z. and Yang G. (2002) Study on intermolecular interactions in supercritical fluids by partial molar volume and compressibility. *J. Supercrit. Fluids* **22**, 15–19.
20. Bailey D. M., Liu C. H., Holste J. C., Hall K. R., Eubank P. T. and Marsh K. M. (1987) Thermodynamic Properties of Pure Hydrogen Sulfide and Mixtures Containing Hydrogen Sulfide with Methane, Carbon Dioxide, Methylcyclohexane and Toluene. *Gas Processors Assoc. Research Report* RR–107.
21. Barry A. O., Kaliaguine S. C. and Ramalho R. S. (1983) Measurement of Enthalpies of Mixing in Gaseous Phase for the Binary System Carbon Dioxide – Hydrogen Sulphide by an Isothermal Flow Calorimeter. *Can. J. Chem. Eng.* **61**, 241–245.
22. Chapoy A., Mohammadi A. H., Chareton A., Tohidi B. and Richon D. (2004) Measurement and Modeling of Gas Solubility and Literature Review of the Properties for the Carbon Dioxide–Water System. *Ind. Eng. Chem. Res.***43**, 1794–1802.
23. Diamond L. W. (2001) Review of the systematics of CO_2 –H_2O fluid inclusions. *Lithos* **55**, 69–99.
24. Diamond L. W. and Akinfiev N. N. (2003) Solubility of CO_2 in water from −1.5 to 100 ◦C and from 0.1 to 100 MPa: evaluation of literature data and thermodynamic modeling. *Fluid Phase Eq.* **208**, 265–290.
25. Duan Z., Hu J., Li D. and Mao S. (2008) Densities of the CO_2–H_2O and CO_2–H_2O–NaCl Systems Up to 647 K and 100 MPa. *Energy Fuels* **22**, 1666–1674.
26. Hu J., Duan Z., Zhu C. and Chou I-M. (2007) PVTx properties of the CO_2–H_2O and CO_2–H_2O–NaCl systems below 647 K: Assessment of experimental data and thermodynamic models. *Chem. Geol.* **238**, 249–267.
27. Longhi J. (2005) Phase equilibria in the system CO_2–H_2O I: New equilibrium relations at low temperatures. *Geochim. Cosmochim. Acta* **69**, 529–539.
28. Paulus M. E. and Penoncello S. G. (2006) Correlation for the Carbon Dioxide and Water Mixture Based on The Lemmon–Jacobsen Mixture Model and the Peng–Robinson Equation of State. *Int. J. Thermophys.* **27**, 1373–1386.
29. Novitskiy A. A., Perez E., Wu W., Ke J. and Poliakoff M. (2009) A New Continuous Method for Performing Rapid Phase Equilibrium Measurements on Binary Mixtures Containing CO_2 or H_2O at High Pressures and Temperatures. *J. Chem. Eng. Data* **54**, 1580–1584.
30. Siqueira-Campos C. E. P., D'Amato-Villardi H. G., Pellegrini-Pessoa F. L. and Cohen-Uller A. M. (2009) Solubility of Carbon Dioxide in Water and Hexadecane: Experimental Measurement and Thermodynamic Modeling. *J. Chem. Eng. Data* **54**, 2881–2886.
31. Bhambhani Y. and Singh, M. 1991 Physiological effects of hydrogen sulfide inhalation during exercise in healthy men. J. Appl. Physiol. 71:1872–1877

8. Tables and Figures

Table 1. Summary compilation of CO_2 specifications [2-13]

Component	Range
CO_2	90 – 99.7%
Argon – Ar	4%
Oxygen – O_2	10 ppm – 4%
Nitrogen – N_2	300 ppm – 4%
Hydrogen – H_2	1 – 4%
Hydrogen sulfide – H_2S	10 ppm to 1.5%
Hydrocarbons – total	1 – 5%
NO_2 or NO_x	100 – 1500 ppm
Particulates	0.1 to 10 mg/Nm^3
Sulfur dioxide – SO_2	2 – 1500 ppm
Sulfur – total	10 – 1450 ppmw
Water – H_2O	0 – 643 ppm

ppm – ppm volume
ppmw – ppm weight

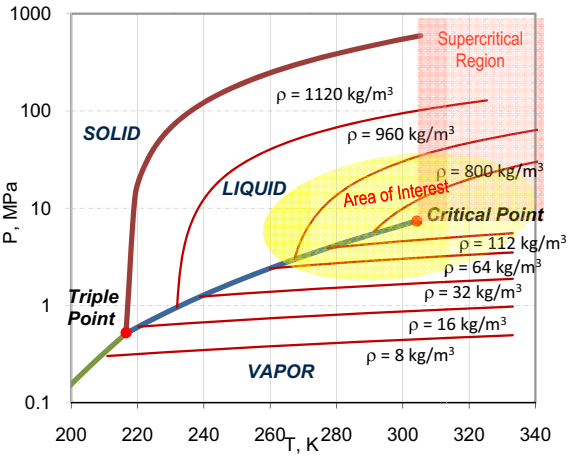

Figure 1: CO_2 phase diagram.

Figure 2: CO_2 injection – simple schematic.

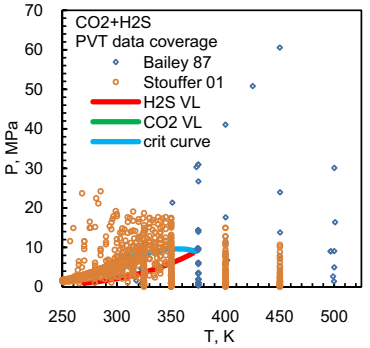

Figure 3: CO_2 + H_2S PVT data coverage.

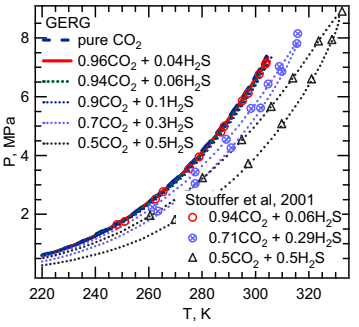

Figure 4: CO_2 + H_2S bubble- and dew-point curves for fixed compositions.

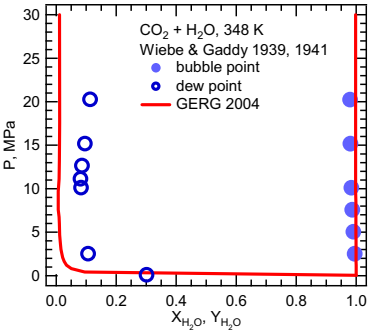

Figure 5: CO_2 + H_2O Vapor-Liquid Equilibrium at 348K.

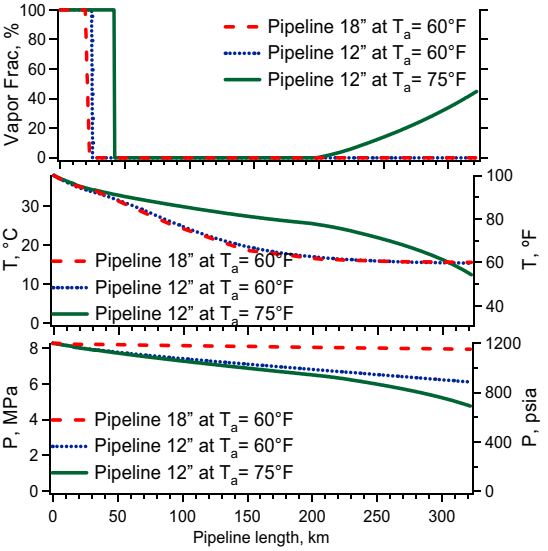

Figure 6: Effect of pipeline diameter and ambient temperature for pure CO_2 stream.

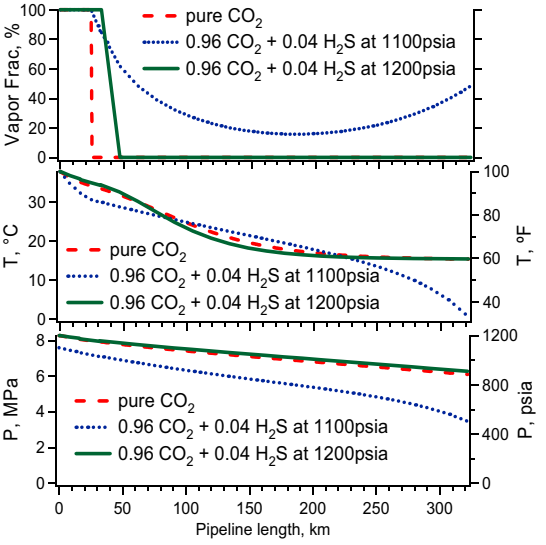

Figure 7: Pipeline model for pure CO_2 and 96%CO_2 + 4%H_2S at 1100 psia and 1200 psia.

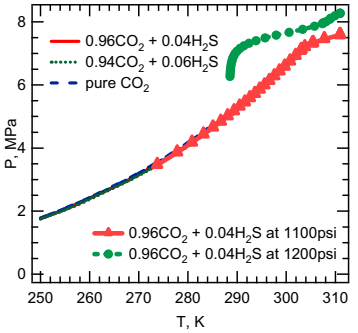

Figure 8: CO_2 + H_2S phase diagram with pipeline model.

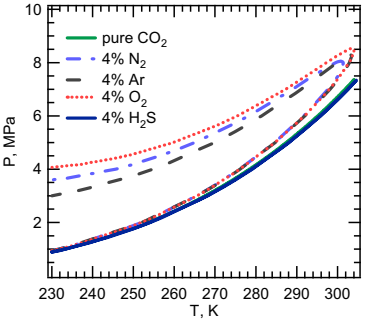

Figure 9: VLE diagram for mixtures of CO_2 with N_2, Ar, O_2, H_2S.